DOI: 10.1002/ejic.201001321

Amine-Templated Cobalt(II) Coordination Polymer Exhibiting Novel Magnetic Properties: Effect of Dehydration

C. M. Nagaraja,[a] Nitesh Kumar,[a] Tapas Kumar Maji,[a,b] and C. N. R. Rao*[a,b]

Keywords: Coordination polymers / Magnetic properties / Cobalt / Hard magnets / Canted antiferromagnets / Hydration

An amine-templated 2D coordination polymer of Co^{II} with the formula $\{[EDAH_2][Co_2F_2(SO_4)_2(H_2O)_2]\}_n$ (**1**) (EDA = ethylenediamine), has been synthesised and structurally characterised. It consists of a 1D chain bridged by F^- ions, which are interconnected by SO_4^{2-} tetrahedra forming a 2D $[Co_2F_2(SO_4)_2(H_2O)_2]_n^{2-}$ corrugated sheet. The diprotonated cation $[EDAH_2]$ is intercalated between the sheets. Temperature-dependent magnetic measurements reveal the presence of spin-canted antiferromagnetism and hard-magnet-like behaviour with large a magnetic hysteresis with a coercive field (H_c) of 16.2 kOe and a remnant magnetisation (M_R) of 1.64 μ_B. The coordinated water molecules in **1** can be removed by heating at 250 °C under vacuum to obtain the dehydrated phase $\{[EDAH_2][Co_2F_2(SO_4)_2]\}_n$ (**1′**), which – upon exposure to water vapour for 24 h – gave the monoaqua compound, $\{[EDAH_2][Co_2F_2(SO_4)_2(H_2O)]\}_n$ (**1′′**). This dehydration/rehydration process is accompanied by a structural transformation and a magnetic phase transition between the spin-canted antiferromagnetic state of the hydrated phase to the antiferromagnetic state of the dehydrated phase.

Introduction

Metal-organic coordination polymers have attracted much attention in the past few years because of their interesting network topologies and novel properties.[1] Among the coordination polymers, those exhibiting long-range magnetic ordering and hard-magnet-like behaviour are of special interest in realising molecular magnetic materials.[2] Compounds exhibiting reversible magnetic phase transitions when subjected to external stimuli such as heat, light or induced by guest molecules could have potential applications as magnetic sensors and switches.[3,4] While there are reports of coordination polymers exhibiting reversible crystal-to-crystal transformations, examples of transformations accompanied by magnetic phase transitions are very rare.[4] In this context, there have been efforts to design magnetic materials with extended structures by using multifunctional bridging ligands, but it is still difficult to predict the structures and the magnetic behaviour of such designed materials.[5] In order to achieve strong magnetic interactions between paramagnetic centres, short bridging ligands such as oxido,[6] cyanido[7] and azido[8] are commonly employed. We have been attempting to synthesise amine-templated transition metal coordination polymers with the Kagomé lattice with novel magnetic properties by incorporating F^- and SO_4^{2-} anions.[9] The SO_4^{2-} anion can take up different bridging modes (μ_1-O1, μ_2-O1, O2, μ_3-O1, O2, O3, or μ_4-O1, O2, O3, and O4) and can efficiently mediate ferromagnetic (FM) and antiferromagnetic (AFM) coupling between metal centres.[10] In continuation of our efforts to synthesise amine-templated magnetic coordination polymers with novel magnetic properties, we have synthesised a 2D coordination polymer of Co^{II} (S = 3/2) by connecting with SO_4^{2-} and F^- anions, with the composition $\{[EDAH_2][Co_2F_2(SO_4)_2(H_2O)_2]\}_n$ (**1**). The compound exhibits a transition from a spin-canted antiferromagnetic state to an antiferromagnetic state triggered by dehydration/rehydration of the coordinated water molecules.

Results and Discussion

Crystal Structure

Compound **1** was prepared under solvothermal conditions at 180 °C. It crystallises in the triclinic space group $P\bar{1}$. The X-ray structure determination reveals that the asymmetric unit consists of two crystallographically independent Co^{II} centres, which are in special positions and bridged by F^- and SO_4^{2-} anions (Figure 1) forming a 2D coordination network lying in the *ab* plane as can be seen from Figure 2a and b. The anionic $[Co_2F_2(SO_4)_2(H_2O)_2]_n^{2-}$ layer is templated by the diprotonated ethylenediamine ($EDAH_2$) cation, which becomes intercalated between the layers as shown in Figure 2c. Two Co^{II} ions are bridged by F^- ions forming a 1D chain along the *b* axis with a Co1–F–Co2 angle of 135.7°. The 1D chains are further con-

[a] Chemistry and Physics of Materials Unit,
Jakkur P. O., Bangalore 560064, India
[b] New Chemistry Unit, Jawaharlal Nehru Centre for Advanced Scientific Research,
Jakkur P. O., Bangalore 560064, India
Fax: +91-80-22082760
E-mail: cnrrao@jncasr.ac.in

Supporting information for this article is available on the WWW under http://dx.doi.org/10.1002/ejic.201001321.

nected by SO_4^{2-} anions resulting in a 2D $[Co_2F_2(SO_4)_2(H_2O)_2]_n^{2-}$ corrugated sheet in the *ab* plane (Figure 2a and b).

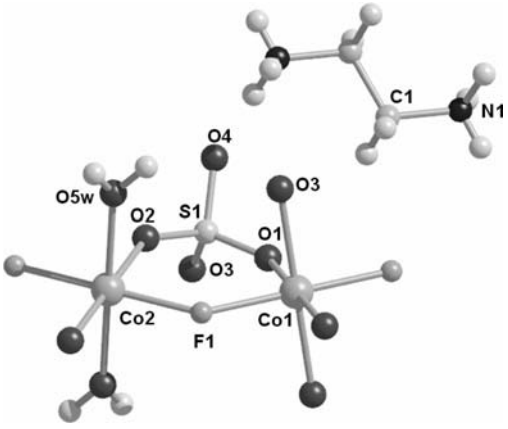

Figure 1. View of the coordination environment around the Co^{II} centre of $\{[EDAH_2][Co_2F_2(SO_4)_2(H_2O)_2]\}_n$.

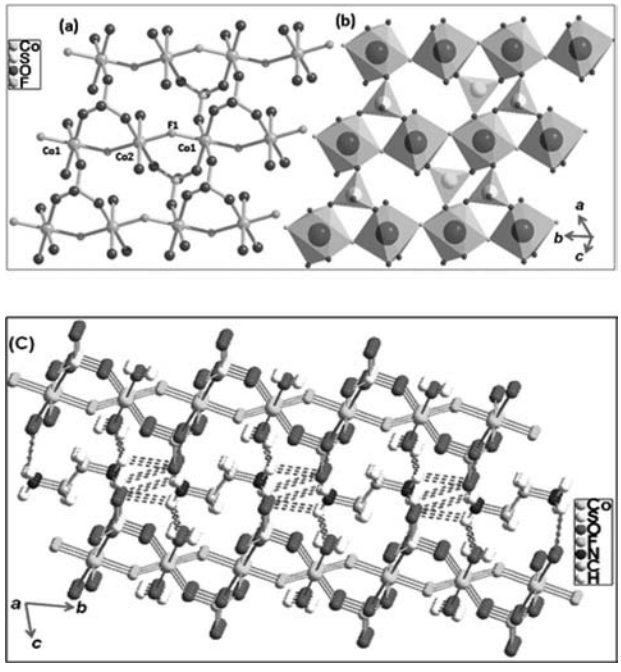

Figure 2. (a) View of the 2D network constructed by the 1D chain of $[Co_2F_2(H_2O)_2]_n$ interconnected by SO_4^{2-}. (b) Polyhedral view of the 2D sheet. (c) Stacking of the 2D sheets along the *c* axis, showing the intercalated protonated ethylenediamine involved in H-bonding with the sheet.

The SO_4^{2-} ion acts as a tridentate bridging ligand connecting two Co1 and one Co2 centres through the O1, O3 and O2 atoms with the O4 atom remaining pendant. The geometry around the Co^{II} centre is a distorted $Co^{II}O_4F_2$ octahedron. The octahedron around Co1 is formed by four oxygen atoms (O1, O1a, O3, and O3a; a = –1 + *x*, *y*, *z*) from the two bridging SO_4^{2-} ions and two F^- anions (F1 and F1a; a = –1 + *x*, *y*, *z*). The octahedron around Co2 is formed from two oxygen atoms (O2 and O2a; a = –1 + *x*, *y*, *z*) of a bridging SO_4^{2-} ion and two F^- anions (F1 and F1a; a = –1 + *x*, *y*, *z*), the remaining two *trans* positions being occupied by two water molecules (O5w and O5wa; a = –1 + *x*, *y*, *z*) as can be seen from Figure 1. The distances between two adjacent Co^{II} centres in the 1D chain along the F^- linker and in the 2D sheet along the SO_4^{2-} bridge are 3.670 and 5.158 Å, respectively. The M^{II}–O bond lengths are in the range 2.112(2)–2.135(3) Å. The corresponding Co^{II}–F bond lengths are in the range 1.9703(17)–1.9997(15) Å. Selected bond lengths and angles are given in Table 1. The protonated ethylenediamine ($EDAH_2$) is involved in a hydrogen-bonding interaction with the oxygen atoms of SO_4^{2-} and F^- anions of the 2D network resulting in a 3D supramolecular framework (Figure 2c, Table S1).

Table 1. Selected bond lengths [Å] and bond angles [°] for **1**.[a]

Co1–F1	1.9997(15)	Co1–O1	2.112(2)
Co1–O3a	2.1250(19)	Co1–O3b	2.1250(19)
Co1–F1d	1.9997(15)	Co1–O1d	2.112(2)
Co2–F1	1.9703(17)	Co2–O2	2.126(2)
Co2–O5W	2.135(3)	Co2–F1c	1.9703(17)
Co2–O2c	2.126(2)	Co2–O5Wc	2.135(3)
F1–Co1–O1	96.20(8)	O5W–Co2–O5Wc	180.00
F1–Co1–O3c	87.62(8)	O1–Co1–O3a	86.47(8)
F1–Co1–O3b	92.38(8)	F1d-Co1–O1	83.81(8)
F1–Co1–F1d	180.00	Co1–F1–Co2	135.72(10)
F1–Co1–O1d	83.81(8)	F1–Co2–O2	91.89(8)
O1–Co1–O3b	93.53(8)	F1–Co2–F1c	180.00
O1–Co1–O1d	180.00	F1–Co2–O5Wc	89.16(9)
F1–Co2–O5W	90.84(9)	F1–Co2–O2c	88.12(8)
O2–Co2–O5W	87.88(10)	O2–Co2–O5Wc	92.12(10)

[a] Symmetry operators: a = 1 + *x*, *y*, *z*; b = 1 –*x*, 1 – *y*, 2 – *z*; c = 2 – *x*, –*y*, 2 – *z*; d = 2 – *x*, 1 – *y*, 2 – *z*.

Magnetic Properties

Variable-temperature magnetic-susceptibility data of a powder sample of **1** were recorded at 500 Oe under zero-field-cooled (ZFC) and field-cooled (FC) conditions (Figure 3). At 300 K, the χT value is 6.44 emu mol^{-1} K, with an effective magnetic moment of 7.2 μ_B per formula unit, which is slightly higher than the spin-only value of 6.54 μ_B expected for two isolated Co^{II} ions, and this is due to the orbital contribution of the octahedral Co^{II} centres.[11] The inverse susceptibility (χ^{-1}) vs. temperature plot between 75–300 K obeys the Curie–Weiss law with a Curie constant *C* of 7.73 cm^3 mol^{-1} K per formula unit and a Weiss temperature θ of –60 K. The larger value of *C* compared with the expected value of 2.7–3.4 emu mol^{-1} K for a Co^{II} (S = 3/2) ion suggests significant orbital contribution.[11] The large negative value of the Weiss temperature confirms dominant antiferromagnetic exchange interactions in the high-temperature region. On lowering the temperature, both the FC and ZFC susceptibilities start raising at 23 K and reach a maximum value of 9.8 emu mol^{-1} suggesting a ferromagnetic exchange interaction between the adjacent Co^{II} centres. Upon further lowering of the temperature the ZFC curve deviates from the FC curve at 18 K, which is in agreement with a peak in the ac susceptibility measurement suggesting that T_c is about 18 K [Figure S1(a)]. The decrease

of ZFC below T_c could be due to antiferromagnetic interactions between the layers or zero-field splitting effects.[3a] The variable-temperature χT plot (Figure S2) shows a gradual decrease until a minimum of 10.5 $cm^3 mol^{-1} K$ at 23.4 K before abruptly rising to a maximum value of 159.3 $cm^3 mol^{-1} K$ at 17.7 K. This behaviour also suggests ferromagnetic ordering in the system. A plot of ZFC susceptibility vs. T at different dc field strengths of 50, 100 and 500 Oe shows a field-dependent behaviour below 20 K indicating spin-canting (Figure S3). Thus, the susceptibility data of **1** can be described in terms of spin-canted antiferromagnetism.[12] The Co^{II} centres in **1** are antiferromagnetically coupled in the 2 D layer, since the Co1–F–Co2 angle is ca. 130° (135.7°) in accordance with the Goodenough–Kanamori–Anderson superexchange rules.[13]

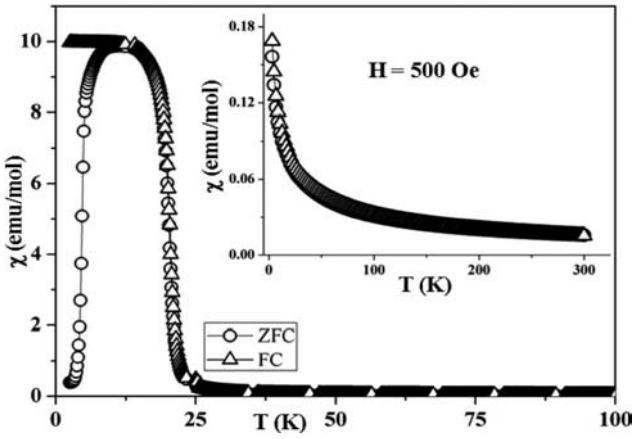

Figure 3. Temperature dependence of the magnetic susceptibility of **1** at 500 Oe under field-cooled (FC) and zero-field-cooled (ZFC) conditions. The inset shows the temperature dependence of the magnetic susceptibility of dehydrated **1′**.

The ferromagnetic-like behaviour observed at low temperatures can arise from spin-canting. In order to fully characterise the ferromagnetic-like behaviour of **1**, isothermal magnetisation with a field up to 50 kOe and magnetic hysteresis were recorded at 3 K (Figure 4). The magnetisation increases gradually at low fields due to antiferromagnetic interactions and increases abruptly at 12.2 kOe due to ferromagnetic interactions. Upon further increase in the applied field, the magnetisation reaches a saturation value of 2.13 μ_B per formula unit at 50 kOe, which is lower than the expected saturation value (Ms = 6 μ_B) for a parallel alignment of two spin-only Co^{II} ions (S = 3/2). This also suggests an antiferromagnetic coupling between the Co^{II} ions. The value of the saturation magnetisation is consistent with the values reported in the literature for spin-canted antiferromagnetic Co^{II} systems.[3a,14] A large hysteresis loop can be observed at 3 K, with a coercive field (H_c) of 16.2 kOe and a remnant magnetisation (M_R) of 1.64 μ_B. The high values of H_c and M_R indicate a hard-magnet-like behaviour of **1**. An H_c value of 52 kOe has been reported in a 1D Co-radical coordination magnet.[15] The magnetic hysteresis in **1** shows kinks, which can arise from anisotropy of the polycrystalline sample since alignment along a particular direction is not achieved during the measurement. A similar magnetic hysteresis with kinks has been reported by Kurmoo et al. in a Co^{II} hydroxide layered structure pillared with *trans*-1,4-cyclohexanedicarboxylato units.[16]

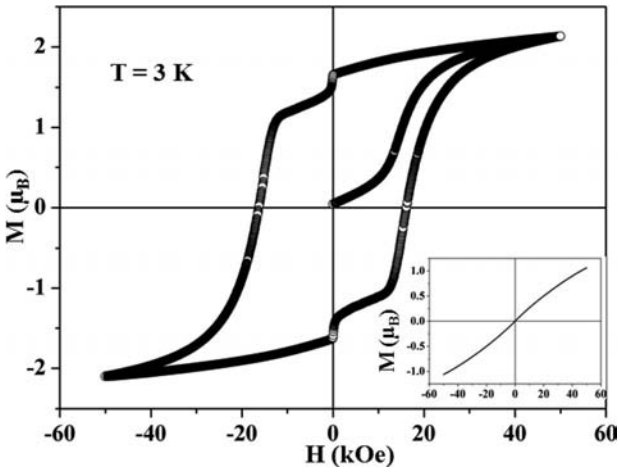

Figure 4. Magnetic hysteresis in **1** at 3 K. The inset shows the M vs. H curve in dehydrated **1′** at 3 K.

The ac magnetic susceptibility measurements of a powder sample of **1** were carried out at H_{ac} = 3 Oe and at different frequencies. Interestingly, both the in-phase (χ') and out-of-phase (χ'') signals display frequency-dependent maxima, suggesting a slow relaxation process (Figure S1). This slow relaxation process could be induced by either domain-wall movements or spin-glass behaviour.[14b]

Dehydration and Rehydration

Thermogravimetric analysis of **1** shows loss of two water molecules around 250 °C (Figure 5). Thus, the dehydrated compound $\{[EDAH_2][Co_2F_2(SO_4)_2]\}_n$ (**1′**) do not show a loss of water molecules at 250 °C. To study the framework stability, a temperature-dependent powder diffraction study

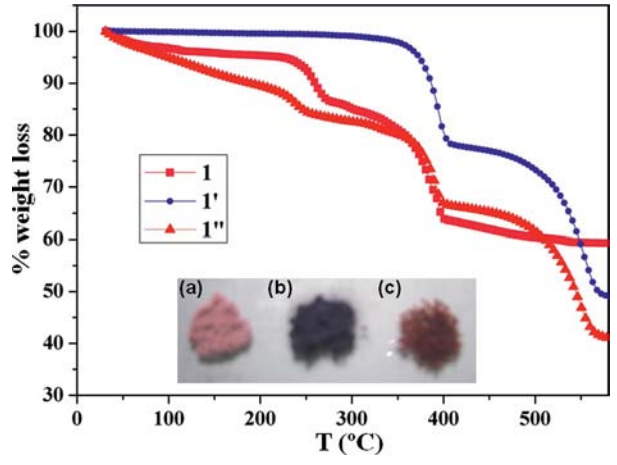

Figure 5. Thermogravimetric curves of as-prepared (**1**) (pink), dehydrated (**1′**) (blue), and mono-aqua (**1′′**) (red) samples. The inset shows photos of the samples **1** (a), **1′** (b), and **1′′** (c).

was carried out (Figure 6). The dehydrated compound **1′** picks up water upon exposure to water vapour for 24 h to give a new hydrated phase, the composition of which matches the monoaqua compound $\{[EDAH_2][Co_2F_2(SO_4)_2(H_2O)]\}_n$ (**1′′**), as confirmed by elemental analysis and TGA (Figure 5). We speculate that the five-coordinate monoaqua compound **1′′** could be stabilised due to the extensive intra- and interlayer hydrogen bonding; as a result the sixth coordination site on the $Co2^{II}$ is not accessible for the coordination of a second water molecule.

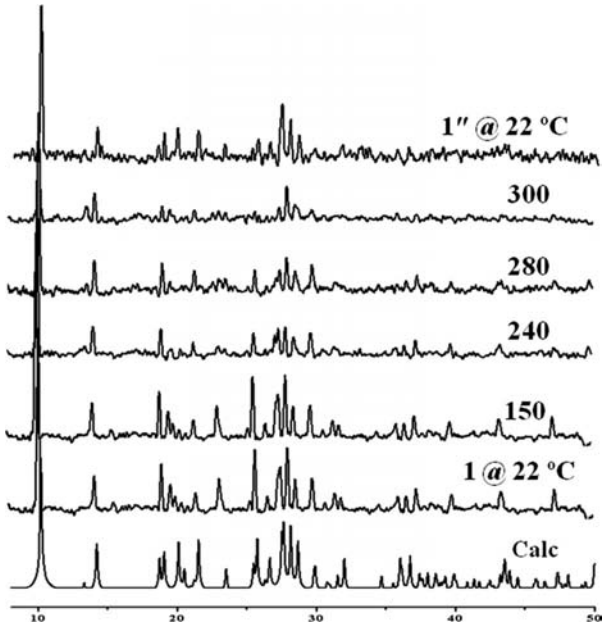

Figure 6. High-temperature powder X-ray diffraction patterns showing the dehydration and rehydration of **1**.

Attempts to determine the single-crystal X-ray structure of **1′** and **1′′** were unsuccessful, since no Bragg spots were observed upon exposure of X-rays to dehydrated and rehydrated crystals, indicating the loss of single-crystallinity upon dehydration/rehydration. However, indexing the powder patterns of dehydrated **1′** and the monoaqua compound **1′′** (Figure 6) by using the TREOR[17] program revealed a change in the crystal system from triclinic to tetragonal and monoclinic with a = 9.750(11) Å, b = 9.750(7) Å, c = 17.600(26) Å, and a = 12.892(10) Å, b = 17.667(8) Å, c = 8.020(3) Å, and β = 101.86° for **1′** and **1′′**, respectively. This clearly shows the occurrence of a structural transformation in **1** upon dehydration and rehydration. The variable-temperature infrared spectra of **1** recorded in situ are shown in Figure 7. At 25 °C, the spectrum shows a band in the region (3300–3500 cm^{-1}) due to O–H stretching modes of the coordinated water molecules and a broad band in the region 2800–3300 cm^{-1}, which is comprised of the hydrogen-bonded N–H stretching modes in the region 3000–3300 cm^{-1} and C–H stretching modes in the region 2800–3000 cm^{-1}. As the sample is heated to 250 °C, the band due to O–H stretching modes of coordinated water molecules disappears. This clearly supports the loss of coordinated water molecules in **1** at 250 °C. The bands in the region 980–1010 cm^{-1} and 1090–1140 cm^{-1} are from ν_1 and ν_3, respectively, of the SO_4^{2-} ion. The bending mode of SO_4^{2-} is in the 450–600 cm^{-1} region. The bending modes of the N–H bonds are also in the expected ranges.[18]

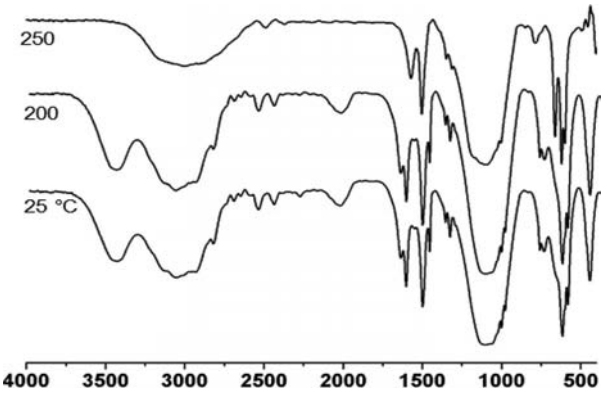

Figure 7. Temperature-dependent infrared spectra showing the dehydration of **1**.

Dehydration of **1** was carried out in a glass tube under vacuum at 250 °C for 5 h. Upon dehydration, the pink colour of **1** turns to blue due to the change in the $Co2^{II}$ coordination from an octahedral to a tetrahedral environment. The rehydration gave a red monoaqua compound; the appearance of the red colour is an indication of $Co2^{II}$ in a square-pyramidal geometry (inset of Figure 5).[19] The diffuse-reflectance solid-state UV/Vis spectrum of **1** shows bands at 513 nm [$^4T_{1g}(F) \rightarrow {}^4T_{1g}(P)$], 675 nm [$^4T_{1g}(F) \rightarrow {}^4A_{2g}(P)$], and 1486 nm [$^4T_{1g}(F) \rightarrow {}^4T_{2g}(F)$], due to the octahedral coordination of Co^{II} ions (Figure S4).[20] The dehydrated **1′** shows a redshift in the absorption maxima at 586 nm [$^4A_2 \rightarrow {}^4T_1(F)$] and 835 nm [$^4A_2 \rightarrow {}^4T_1(P)$] due to the tetrahedral environment of $Co2^{II}$. Similar redshifts in the absorption bands upon changes in the Co^{II} coordination from octahedral to tetrahedral have been reported.[21] The monoaqua compound **1′′** shows bands at 527 nm, 673 nm and 1487 nm due to the octahedral $Co1^{II}$ and additional bands at 857 nm and 1200 nm, which are due to the square-pyramidal $Co2^{II}$ (Figure S4).[22]

Variable-temperature ZFC and FC magnetic susceptibility data of dehydrated **1′** recorded at 500 Oe are shown in the inset of Figure 3. At 300 K, the values of χT and μ_{eff} are 4.71 $cm^3 mol^{-1} K$ and 6.16 μ_B per Co^{II}_2 unit, respectively, being slightly lower than those of parent compound **1**. The inverse susceptibility (χ^{-1}) vs. temperature plot between 75 and 300 K obeys the Curie–Weiss law with C = 6.45 $cm^3 mol^{-1} K$ per formula unit and θ = –115 K. The larger negative value of θ in **1′** compared with that of hydrated **1** indicates dominant antiferromagnetic exchange interactions between the Co^{II} ions, which can be attributed to the change in the coordination environment around the Co2 centre. As the temperature is lowered, both the ZFC and FC susceptibilities increase but show no phase transition above 3 K indicating a loss of ferromagnetic ordering present in **1** upon dehydration (see inset of Figure 3). The

χT vs. T plot (Figure S5) shows a continuous decrease until a minimum of 0.5 $cm^3 mol^{-1} K$ at 3.32 K, due to antiferromagnetic exchange interactions. This is confirmed by the M vs. H curve, which shows the loss of magnetic hysteresis (see the inset of Figure 4). A similar observation of a ferromagnetic to a paramagnetic transition upon loss of guest water molecules has been reported in the Co^{II} coordination framework compound $[Co_3(OH)_2(C_2O_4)_2]\cdot 3H_2O$.[23]

Magnetic behaviour of the monoaqua compound **1**′′ is similar to that of the prepared compound **1** as shown in Figure 8. At 300 K, the values of χT and μ_{eff} are 5.1 $cm^3 mol^{-1} K$ and 6.4 μ_B per $Co^{II}{}_2$ unit, respectively, being slightly lower than those of parent compound **1** and higher than those of dehydrate **1**′. The inverse susceptibility (χ^{-1}) vs. temperature plot between 75 and 300 K obeys the Curie–Weiss law with C = 6.14 $cm^3 mol^{-1} K$ per formula unit and θ = –76 K. The larger negative value of θ compared with that of **1** indicates dominant antiferromagnetic exchange interactions between the Co^{II} ions. As the temperature is lowered, both the FC and ZFC susceptibilities increase starting at 23 K and reaching a maximum value of 3.66 emu mol^{-1} suggesting a ferromagnetic exchange interaction between the adjacent Co^{II} centres. Upon further lowering of the temperature, the ZFC curve deviates from the FC curve at 12.5 K. The χT vs. T plot (Figure S6) shows a gradual decrease until a minimum of 2.90 $cm^3 mol^{-1} K$ at 29.1 K before suddenly rising to a maximum value of 48.38 $cm^3 mol^{-1} K$ at 15.5 K suggesting a ferromagnetic ordering in the system. This is further confirmed by the M vs. H curve at 3 K, which shows a hysteresis loop with an H_c value of 6.5 kOe and an M_R value of 0.34 μ_B. The lower values of H_c and M_R compared with those of the parent compound **1** can be attributed to the change in the coordination environment of $Co2^{II}$, i.e. the presence of one coordinated water molecule as opposed to two in **1**.

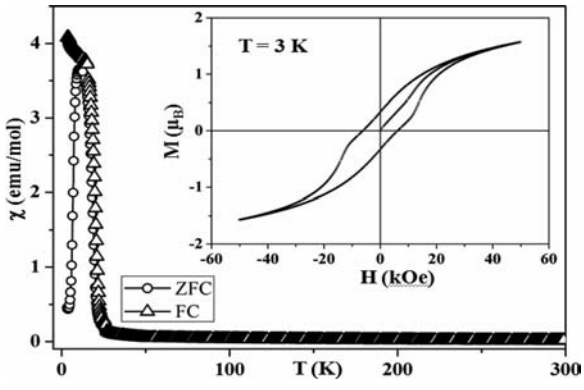

Figure 8. Temperature dependence of the magnetic susceptibility of **1**′′ at 500 Oe under field-cooled (FC) and zero-field-cooled (ZFC) conditions. The inset shows the temperature dependence of the magnetic susceptibility of dehydrated **1**′′.

The magnetic properties of **1** can be explained by considering a spin-canting structure. For an extended system with no inversion centre between adjacent metal ions, spin-canting can arise because of structural anisotropy and anisotropic Dzyaloshinsky–Moriya interactions.[24] The latter tends to orient the neighbouring spins perpendicular to each other. In **1**, the two crystallographically distinct Co^{II} ions in a pseudo-octahedral environment with no inversion centre between the adjacent metal centres, along with the local anisotropy, favours spin-canting at low temperatures. The antiferromagnetically coupled spins between the adjacent metal centres in the 2D sheet are not perfectly antiparallel leading to a ferromagnetic-like behaviour at low temperatures. The thermal energy is not sufficient to overcome spin-canting at low temperatures. Thus, the strong ferromagnet-like behaviour of **1** can be ascribed to the large single-ion magnetic anisotropy of Co^{II}, which arises due to first-order spin-orbit coupling.[25]

Conclusions

We have been able to prepare and characterize a 2D coordination polymer, $\{[EDAH_2][Co_2F_2(SO_4)_2(H_2O)_2]\}_n$ (**1**), with novel magnetic properties. It consists of 2D corrugated $[Co_2F_2(SO_4)_2(H_2O)_2]_n{}^{2-}$ sheets, formed by $[Co–F–Co]_n$ 1D chains interconnected by $SO_4{}^{2-}$ tetrahedra, and templated by diprotonated $[EDAH_2]$ cations. Variable-temperature magnetic properties reveal a spin-canted antiferromagnetism due to magnetic anisotropy and Dzyaloshinsky–Moriya interaction. **1** shows a hard-magnet-like behaviour, which arises from the large local magnetic anisotropy and the high spin moment of Co^{II} (S = 3/2). The coordinated water molecules in **1** are removed upon heating giving rise to a dehydrated phase causing a structural transition and change in coordination of Co^{II}. Rehydration led to the isolation of a monoaqua compound, which is probably stabilised due to extensive hydrogen-bonding interactions. The magnetic phase transition between the spin-canted antiferromagnetic state to an antiferromagnetic state is triggered by the dehydration/rehydration process.

Experimental Section

Materials and Physical Methods: All the starting materials were commercially available and used as received without further purification. Elemental analyses were carried out with a Thermo Scientific Flash 2000 CHN analyser. Thermogravimetric analyses (TGA) were carried out with Mettler Toledo TGA850 instrument in the temperature range of 25–700 °C under nitrogen (flow rate 50 mL min^{-1}) at a heating rate of 3 °C min^{-1}. IR spectra of the compounds were recorded with a Bruker IFS 66v/S spectrophotometer by using KBr pellets in the region 4000–400 cm^{-1}. Powder XRD patterns were measured with a Bruker D8 discover instrument by using Cu-K_α radiation. The pattern agreed with that calculated for the single-crystal structure. Solid-state UV/Vis (reflectance) spectra were recorded with a Perkin–Elmer Model Lambda 900 spectrophotometer. The dc magnetic susceptibility measurements were carried out with a Vibrating Sample Magnetometer, PPMS (Physical Property Measurement System, Quantum Design, USA) in the temperature range 3–300 K with an applied field of

500 Oe. Field variation (–5 kOe to 5 kOe) magnetisation measurements were carried out at 3 K. Diamagnetic corrections were applied by using Pascal's constants. The ac susceptibility measurements were carried out with a SQUID magnetometer.

Synthesis and Characterisation: Compound **1** was synthesised by employing solvothermal conditions at 180 °C in the presence of ethylenediamine. $CoCl_2{\cdot}6H_2O$ (0.237 g, 1 mmol) was dissolved in an ethylene glycol (EG)/water mixture (4.6:0.9 mL) under constant stirring. To this mixture were added sulfuric acid (H_2SO_4, 98%, 0.16 mL, 3 mmol) and ethylenediamine (0.266 mL, 4 mmol), followed by HF (48%, 0.17 mL, 10 mmol). The mixture with the molar composition $CoCl_2{\cdot}6H_2O/H_2SO_4$/EDA/HF/EG/$H_2O$ (1:3:4:10:90:50) was stirred for 1 h and then placed in a 23 mL PTFE-lined acid digestion bomb and heated at 180 °C for 3 d. After cooling to room temperature, pink needle-like crystals of **1** were isolated. Yield 0.289 g (65%). $C_2H_{14}Co_2F_2N_2O_{10}S_2$ (446.12): calcd. C 5.38, H 3.16, N 6.28; found C 5.40, H 2.98, N 6.30. The dehydrated compound **1′** was obtained upon heating of compound **1** to 250 °C under vacuum for 5 h in a glass tube with a stopper. During this period the pink compound turned blue. The monoaqua compound **1′′** was obtained upon exposing the dehydrated compound **1′** to water vapour for 24 h. During this period the blue compound turned reddish. $C_2H_{12}Co_2F_2N_2O_9S_2$ (428.12): calcd. C 5.61, H 2.82, N 6.54; found C 5.58, H 2.80, N 6.45. The TGA curve of **1** shows a weight loss of 8.2% (calcd. 8.1 wt.-%) around 250–300 °C, which corresponds to the loss of two coordinated water molecules. The second-step loss of 18.4% (calcd. 18.1 wt.-%) in the range 320–410 °C corresponds to loss of protonated ethylenediamine and a fluorine atom. The compound then decomposes to unidentified products. Dehydrated **1′** shows a weight loss of 19.4% (calcd. 19.8 wt.-%) around 350–420 °C due to the loss of protonated ethylenediamine and a fluorine atom. The monoaqua compound **1′′** shows a weight loss of 4.2% (calcd. 4.0 wt.-%) around 250–300 °C, which corresponds to the loss of a coordinated water molecule. The second loss of 18.4% (calcd. 18.1 wt.-%) in the range 320–410 °C corresponds to loss of protonated ethylenediamine and a fluorine atom (Figure 5).

X-ray Crystallography: A single crystal of **1** suitable for X-ray diffraction was carefully selected after examination under an optical microscope and then mounted on a thin glass fibre with commercially available super glue. The structural data were collected with a CrysAlis CCD, Oxford Diffractometer with an X-ray generator at 49.30 kV and 0.980 mA, by using Mo-K_α radiation (λ = 0.7107 Å). The cell refinement and the data reduction were carried out in CrysAlis RED.[26] An empirical absorption correction was made by using the SADABS program.[27] The structure was solved by using SIR-92 and refined by a full-matrix least-squares method by using SHELXL.[28] Non-hydrogen atoms were refined anisotropically and hydrogen atoms were fixed by HFIX and placed in ideal positions. All the calculations were carried out by using SHELXL97,[29] PLATON,[30] SHELXS97[31] and the WinGX system (ver. 1.70.01).[32] Details of the structure determination and final refinements are summarised in Table 2. Selected bond lengths and angles are given in Table 1. CCDC-804762 contains the supplementary crystallographic data for this paper. This data can be obtained free of charge from The Cambridge Crystallographic Data Centre via www.ccdc.cam.ac.uk/data_request/cif.

Supporting Information (see footnote on the first page of this article): Tables of hydrogen bond lengths and angles, ac susceptibility data, variable-temperature dc susceptibility (ZFC) data of **1**, χT vs. T plot and diffuse-reflectance solid-state UV/Vis spectra of **1**, **1′** and **1′′**.

Table 2. Crystal and structure refinement data for **1**.

Empirical formula	CH_7CoFNO_5S
Formula mass	221.05
Crystal system	triclinic
Space group	$P\bar{1}$ (no. 2)
a [Å]	5.0279(5)
b [Å]	7.3545(7)
c [Å]	9.1029(7)
α [°]	72.415(7)
β [°]	85.269(7)
γ [°]	70.878(9)
V [Å]^3	303.12(5)
T [K]	293(2)
Z	2
$D_{calcd.}$ [g cm^{-3}]	2.422
μ [mm^{-1}]	3.161
$F(000)$	224
Reflections observed/unique	6556/2248
R_1[a]/wR_2[b] [$I > 2\sigma(I)$]	0.0271/0.0705

[a] $R_1 = \Sigma(|F_o| - |F_c|)/\Sigma|F_o|$. [b] $wR_2 = [\Sigma w(|F_o| - |F_c|)^2/\Sigma w|F_o|^2]^{1/2}$.

Acknowledgments

We thank Dr. A. Sundaresan and Dr. S. K. Pati for useful discussions. C. M. N. thanks the Defence Research and Development Organisation (DRDO), India, for a fellowship.

[1] a) B. Moulton, M. J. Zaworotko, *Chem. Rev.* **2001**, *101*, 1629; b) O. M. Yaghi, M. O. Keeffe, N. W. Ockwig, H. K. Chae, M. Eddaoudi, J. Kim, *Nature* **2003**, *423*, 705; c) C. N. R. Rao, S. Natarajan, R. Vaidhyanathan, *Angew. Chem. Int. Ed.* **2004**, *43*, 1466; d) S. Kitagawa, R. Kitaura, S. Noro, *Angew. Chem. Int. Ed.* **2004**, *43*, 2334.

[2] a) O. Kahn, *Molecular Magnetism*, VCH, New York, **1993**; b) *Magnetism: Molecules to Materials* (Eds.: J. S. Miller, M. Drilon), Willey-VCH, Weinheim, **2002–2005**, vol. I–V; c) J. S. Miller, *Adv. Mater.* **2002**, *14*, 1105; d) D. Gatteschi, R. Sessoli, *Angew. Chem. Int. Ed.* **2003**, *42*, 268.

[3] a) X.-N. Cheng, W.-X. Zhang, X.-M. Chen, *J. Am. Chem. Soc.* **2007**, *129*, 15738; b) W.-W. Sun, C.-Y. Tian, X.-H. Jing, Y.-Q. Wang, E.-Q. Gao, *Chem. Commun.* **2009**, 4741; c) M. Seredyuk, A. B. Gaspar, V. Ksenofontov, M. Verdaguer, F. Villain, P. Gütlich, *Inorg. Chem.* **2009**, *48*, 6130; d) Y.-M. Legrand, A. van der Lee, N. Masquelez, P. Rabu, M. Barboiu, *Inorg. Chem.* **2007**, *46*, 9083; e) B. Nowicka, M. Rams, K. Stadnicka, B. Sieklucka, *Inorg. Chem.* **2007**, *46*, 8123; f) M. Nihei, L. Han, H. Oshio, *J. Am. Chem. Soc.* **2007**, *129*, 5312.

[4] a) Y. Yoshida, K. Inoue, M. Kurmoo, *Inorg. Chem.* **2009**, *48*, 267; b) Y.-J. Zhang, T. Liu, S. Kanegawa, O. Sato, *J. Am. Chem. Soc.* **2009**, *131*, 7942; c) W. Kaneko, M. Ohba, S. Kitagawa, *J. Am. Chem. Soc.* **2007**, *129*, 13706; d) X.-N. Cheng, W.-X. Zhang, Y.-Y. Lin, Y.-Z. Zheng, X.-M. Chen, *Adv. Mater.* **2007**, *19*, 1494.

[5] a) T. Kajiwara, A. Kamiyama, T. Ito, *Chem. Commun.* **2002**, 1256; b) D. Maspoch, D. Ruiz-Molina, K. Wurst, N. Domingo, M. Cavallini, F. Biscarini, J. Tejada, C. Rovira, J. Veciana, *Nat. Mater.* **2003**, *2*, 190; c) J. R. Galán-Mascarós, K. R. Dunbar, *Angew. Chem. Int. Ed.* **2003**, *42*, 2289; d) D. Maspoch, D. Ruiz-Molina, J. Veciana, *J. Mater. Chem.* **2004**, *14*, 2713; e) R. D. Poulsen, A. Bentien, M. Chevalier, B. B. Iversen, *J. Am. Chem. Soc.* **2005**, *127*, 9156.

[6] a) H. A. Hesham, J. Sanchiz, C. Janiak, *Dalton Trans.* **2008**, *36*, 4877; b) D. Armentano, G. D. Munno, T. F. Mastropietro, M. Julve, F. Lloret, *J. Am. Chem. Soc.* **2005**, *127*, 10778.

[7] a) J. H. Yoon, H. S. Yoo, H. C. Kim, S. W. Yoon, B. J. Suh, C. S. Hong, *Inorg. Chem.* **2009**, *48*, 816; b) E. Colacio, I. B.

Maimoun, F. Lloret, J. Suarez-Varela, *Inorg. Chem.* **2005**, *44*, 3771.

[8] a) Y. Ma, J.-Y. Zhang, A.-L. Cheng, Q. Sun, E.-Q. Gao, C.-M. Liu, *Inorg. Chem.* **2009**, *48*, 6142; b) J. D. Woodward, R. V. Backov, K. A. Abboud, D. Dai, H.-J. Koo, M.-H. Whangbo, M. W. Meisel, D. R. Talham, *Inorg. Chem.* **2005**, *44*, 638; c) Y.-Z. Zhang, S. Gao, H.-L. Sun, G. Su, Z.-M. Wang, S.-W. Zhang, *Chem. Commun.* **2004**, 1906.

[9] a) C. M. Nagaraja, J. N. Behera, T. K. Maji, S. K. Pati, C. N. R. Rao, *Dalton Trans.* **2010**, *39*, 6947; b) S. K. Pati, C. N. R. Rao, *Chem. Commun.* **2008**, 4683; c) G. Paul, A. Choudhury, E. V. Sampathkumaran, C. N. R. Rao, *Angew. Chem. Int. Ed.* **2002**, *41*, 4297; d) C. N. R. Rao, G. Paul, A. Choudhury, E. V. Sampathkumaran, A. K. Raychaudhuri, S. Ramasesha, I. Rudra, *Phys. Rev. B* **2003**, *67*, 134425; e) J. N. Behera, G. Paul, A. Choudhury, C. N. R. Rao, *Chem. Commun.* **2004**, 456; f) C. N. R. Rao, E. V. Sampathkumaran, R. Nagarajan, G. Paul, J. N. Behera, A. Choudhury, *Chem. Mater.* **2004**, *16*, 1441; g) J. N. Behera, C. N. R. Rao, *J. Am. Chem. Soc.* **2006**, *128*, 9334.

[10] a) C. N. R. Rao, J. N. Behera, M. Dan, *Chem. Soc. Rev.* **2006**, *35*, 375; b) J. N. Behera, C. N. R. Rao, *Chem. Asian J.* **2006**, *1*, 742.

[11] M. Kurmoo, *Chem. Soc. Rev.* **2009**, *38*, 1353.

[12] a) S. Vilminot, G. André, F. Bourée-Vigneron, P. J. Baker, S. J. Blundell, M. Kurmoo, *J. Am. Chem. Soc.* **2008**, *130*, 13490; b) S. O. H. Gutschke, D. J. Price, A. K. Powell, P. T. Wood, *Angew. Chem. Int. Ed.* **1999**, *38*, 1088; c) H.-P. Jia, W. Li, Z.-F. Ju, J. Zhang, *Chem. Commun.* **2008**, 371.

[13] R. Skomski, *Simple Models of Magnetism*, Oxford University Press, Oxford, **2008**.

[14] a) X.-N. Cheng, W. Xue, X.-M. Chen, *Eur. J. Inorg. Chem.* **2010**, 3850; b) D.-K. Cao, Y.-Z. Li, L.-M. Zheng, *Inorg. Chem.* **2007**, *46*, 7571.

[15] N. Ishii, Y. Okamura, S. Chiba, T. Nogami, T. Ishida, *J. Am. Chem. Soc.* **2008**, *130*, 24.

[16] M. Kurmoo, H. Kumagai, S. M. Hughes, C. J. Kepert, *Inorg. Chem.* **2003**, *42*, 6709.

[17] P.-E. Werner, L. Eriksson, M. Westdahl, *J. Appl. Crystallogr.* **1985**, *18*, 367.

[18] K. Nakamato, *Infrared and Raman Spectra of Inorganic and Coordination Compounds*, Wiley-Interscience, New York, **1978**.

[19] J. K. Stalick, P. W. R. Corfield, D. W. Meek, *Inorg. Chem.* **1973**, *7*, 1668.

[20] a) A. B. P. Lever, *Inorganic Electronic Spectroscopy*, 2nd ed., Elsevier, Amsterdam, **1984**; b) S.-I. Aizawa, S. Funahashi, *Inorg. Chem.* **2002**, *41*, 4555.

[21] J. A. Botas, G. Calleja, M. Sánchez-Sánchez, M. G. Orcajo, *Langmuir* **2010**, *26*, 5300.

[22] C. Zimmermann, F. W. Heinemann, A. Grohmann, *Eur. J. Inorg. Chem.* **2005**, 3506.

[23] M. Kurmoo, H. Kumagai, K. W. Chapmanc, C. J. Kepert, *Chem. Commun.* **2005**, 3012.

[24] a) I. Dzyaloshinsky, *J. Phys. Chem. Solids* **1958**, *4*, 241; b) T. Moriya, *Phys. Rev.* **1960**, *120*, 91; c) T. Moriya, *Phys. Rev.* **1960**, *117*, 635; d) R. L. Carlin, *Magnetochemistry*, Springer-Verlag, Berlin, **1986**.

[25] J.-R. Li, Q. Yu, Y. Tao, X. H. Bua, J. Ribasb, S. R. Batten, *Chem. Commun.* **2007**, 2290.

[26] Oxford Diffraction, *CrystAlis CCD and CrystAlis RED*, version 1.171.33.31, Oxford Diffraction Ltd., Abingdon, Oxfordshire, England, **2009**.

[27] G. M. Sheldrick, *SADABS User Guide*, University of Göttingen, Göttingen, Germany, **1993**.

[28] A. Altomare, G. Cascarano, C. Giacovazzo, A. Gualaradi, *J. Appl. Crystallogr.* **1993**, *26*, 343.

[29] G. M. Sheldrick, *SHELXL97, Program for the Solution of Crystal Structure*, University of Göttingen, Göttingen, Germany, **1997**.

[30] A. L. Spek, *J. Appl. Crystallogr.* **2003**, *36*, 7.

[31] G. M. Sheldrick, *SHELXS97, Program for the Solution of Crystal Structure*, University of Göttingen, Göttingen, Germany, **1997**.

[32] *WinGX, A Windows Program for Crystal Structure Analysis*: L. J. Farrugia, *J. Appl. Crystallogr.* **1999**, *32*, 837.

Received: December 16, 2010
Published Online: March 29, 2011

